RIA-78-U179

AD

ARBRL-MR-02808

BRL

MEMORANDUM REPORT ARBRL-MR-02808

EXPERIMENTAL MEASUREMENTS IN THE TURBULENT BOUNDARY LAYER OF A YAWED, SPINNING OGIVE-CYLINDER BODY OF REVOLUTION AT MACH 3.0. PART I. DESCRIPTION OF THE EXPERIMENT AND DATA ANALYSIS

Lyle D. Kayser
Walter B. Sturek

TECHNICAL
LIBRARY

January 1978

19971010 148

Approved for public release; distribution unlimited.

DTIC QUALITY INSPECTED 3

USA ARMAMENT RESEARCH AND DEVELOPMENT COMMAND
USA BALLISTIC RESEARCH LABORATORY
ABERDEEN PROVING GROUND, MARYLAND

Destroy this report when it is no longer needed.
Do not return it to the originator.

Secondary distribution of this report by originating or sponsoring activity is prohibited.

Additional copies of this report may be obtained from the National Technical Information Service, U.S. Department of Commerce, Springfield, Virginia 22161.

The findings in this report are not to be construed as an official Department of the Army position, unless so designated by other authorized documents.

The use of trade names or manufacturers' names in this report does not constitute indorsement of any commercial product.

UNCLASSIFIED

SECURITY CLASSIFICATION OF THIS PAGE (When Data Entered)

REPORT DOCUMENTATION PAGE

READ INSTRUCTIONS BEFORE COMPLETING FORM

1. REPORT NUMBER
MEMORANDUM REPORT ARBRL-MR-02808

2. GOVT ACCESSION NO.

3. RECIPIENT'S CATALOG NUMBER

4. TITLE (and Subtitle)
EXPERIMENTAL MEASUREMENTS IN THE TURBULENT BOUNDARY LAYER OF A YAWED, SPINNING OGIVE-CYLINDER BODY OF REVOLUTION AT MACH 3.0. PART I. DESCRIPTION OF THE EXPERIMENT AND DATA ANALYSIS

5. TYPE OF REPORT & PERIOD COVERED
Final

6. PERFORMING ORG. REPORT NUMBER

7. AUTHOR(s)
Lyle D. Kayser
Walter B. Sturek

8. CONTRACT OR GRANT NUMBER(s)

9. PERFORMING ORGANIZATION NAME AND ADDRESS
USA Ballistic Research Laboratory
(ATTN: DRDAR-BLL)
Aberdeen Proving Ground, MD 21005

10. PROGRAM ELEMENT, PROJECT, TASK AREA & WORK UNIT NUMBERS
RDT&E 1L161102AH43

11. CONTROLLING OFFICE NAME AND ADDRESS
US Army Armament Research & Development Command
US Army Ballistic Research Laboratory
(ATTN: DRDAR-BL)
Aberdeen Proving Ground, MD 21005

12. REPORT DATE
JANUARY 1978

13. NUMBER OF PAGES
33

14. MONITORING AGENCY NAME & ADDRESS (if different from Controlling Office)

15. SECURITY CLASS. (of this report)
Unclassified

15a. DECLASSIFICATION/DOWNGRADING SCHEDULE

16. DISTRIBUTION STATEMENT (of this Report)
Approved for public release; distribution unlimited.

17. DISTRIBUTION STATEMENT (of the abstract entered in Block 20, if different from Report)

18. SUPPLEMENTARY NOTES

19. KEY WORDS (Continue on reverse side if necessary and identify by block number)
Turbulent Boundary Layers
Yawed Spinning Bodies
Experimental Measurements
Supersonic Flow

20. ABSTRACT (Continue on reverse side if necessary and identify by block number) (1cb)

Many projectiles used by the Army are slender, spin stabilized bodies of revolution. The distorted boundary layer, which results from a spinning body at angle of yaw, generates Magnus forces and moments. The BRL is conducting and supporting theoretical and experimental Magnus research efforts. Experimental results of surveys of the turbulent boundary layer on a secant-ogive-cylinder at angles of attack up to 6 degrees for spin rates of 0 and 333 rps at Mach = 3 are presented in this report. Limited comparisons of the data

(Continued)

DD FORM 1 JAN 73 1473 EDITION OF 1 NOV 65 IS OBSOLETE

UNCLASSIFIED

SECURITY CLASSIFICATION OF THIS PAGE (When Data Entered)

20. ABSTRACT (Continued):

to finite-difference three-dimensional boundary layer computations indicate encouraging agreement. The theory is shown to accurately model the effects of surface spin and the main effects of surface spin are shown to occur near the lee side of the model. Complete data tabulations are provided in Part II to facilitate their use for comparison to theoretical computations.

TABLE OF CONTENTS

		Page
	LIST OF ILLUSTRATIONS	5
I.	INTRODUCTION	7
II.	EXPERIMENT	8
III.	DISCUSSION OF RESULTS	10
IV.	CONCLUDING REMARKS	12
	REFERENCES	27
	LIST OF SYMBOLS	29
	DISTRIBUTION LIST	31

LIST OF ILLUSTRATIONS

Figure		Page
1.	Model Geometry	13
2.	Model Installation Photograph	14
3.	Shadowgraph, α = 4.2 Degrees, Z/D = 3.33	15
4.	Surface Pressure Distribution on the SOC Model	16
5.	Model Coordinate System	17
6.	Velocity Profiles, Theory Compared With Experiment	18
7.	Velocity Profiles, Theory Compared With Experiment	19
8.	Experimental Velocity Profiles, Effects of Spin	20
9.	Boundary Layer Displacement Thickness, δ_x^*, Theory and Experiment	21
10.	Increment of Displacement Thickness, $\Delta\delta_x^*$, Due to Spin	22
11.	Preston Tube Skin Friction Results	23
12.	Experimental Displacement Thicknesses, α = 6.3 Degrees	24

I. INTRODUCTION

Many projectiles used by the Army are slender, spin stabilized bodies of revolution. The distorted boundary layer, which results from a spinning body at angle of yaw, generates Magnus forces and moments. Recent Army interest in achieving increased range and greater payload capacity in artillery projectiles has led to designs with long, slender ogives, increased projectile length, and boattailed afterbodies. These designs have resulted in decreased drag and an increase in range; however, the gyroscopic stability of these shapes is less than that of more conventional designs. This means that these new shapes are more susceptible to a Magnus induced instability. The Magnus force is small, typically 1/10 to 1/100 of the normal force; however, its effect is important because the Magnus moment acts to undamp the projectile throughout its flight. Thus, it is desirable to minimize the Magnus moment so that the projectile flies at a small average angle of attack and achieves the greatest range capability.

BRL has developed numerical techniques for computing Magnus effects (forces and moments) which result from spin induced distortion of the boundary layer. The computational procedure is described in references 1, 2, 3, and 4 and consists of numerical techniques for computing: (1) the three dimensional supersonic inviscid flow over a yawed body of revolution; (2) the three dimensional laminar/turbulent boundary layer development over a yawed, spinning body of revolution; (3) the three dimensional boundary layer displacement surface; and (4) the three dimensional supersonic flow over a yawed body plus three dimensional boundary layer displacement surface to yield pitch and yaw

---

1. *H. A. Dwyer, "Three Dimensional Flow Studies Over a Spinning Cone at Angle of Attack," BRL Contract Report No. 137, February 1974, U.S. Army Ballistic Research Laboratory, Aberdeen Proving Ground, Maryland. AD 774795.*

2. *H. A. Dwyer and B. R. Sanders, "Magnus Forces on Spinning Supersonic Cones. Part I: The Boundary Layer," BRL Contract Report No. 248, July 1975, U.S. Army Ballistic Research Laboratory, Aberdeen Proving Ground, Maryland. AD A013518. Also AIAA Journal, Vol. 14, No. 4, April 1976, p. 498.*

3. *B. R. Sanders, "Three-Dimensional, Steady, Inviscid Flow Field Calculations With Application to the Magnus Problem," PhD Dissertation, University of California, Davis, California, May 1974.*

4. *W. B. Sturek (et al), "Computations of Turbulent Boundary Layer Development Over a Yawed, Spinning Body of Revolution With Application to Magnus Effect," BRL Report No. 1985, May 1977, U.S. Army Ballistic Research Laboratory, Aberdeen Proving Ground, Maryland. AD A041338.*

plane aerodynamic coefficients. Experimental studies are being carried out to provide data which will help guide this theoretical effort. The purpose of the experimental measurements reported here is to provide data to evaluate the theoretical computations of turbulent boundary layer development. The objective of this report is to provide a summary of the boundary layer profile data with some analysis and comparison with theory. A complete tabulation of experimental data is presented in Part II of this report (reference 5).

II. EXPERIMENT

All experimental results presented in this report were obtained on the secant-ogive-cylinder model (SOC) shown in Figure 1. The model is 57.15 mm (2.25 inches) in diameter and 342.9mm (13.5 inches) long. A boundary layer trip was placed on the ogive to insure the location of the start of turbulent flow. The tests were conducted in the BRL Supersonic Wind Tunnel No. 1 which is a continuous flow tunnel with a test section of 330 x 381 mm (13 x 15 inches). Measurements of the total head pressure through the boundary layer were made with a flattened impact pressure probe 1.5 mm wide by 0.15 mm high. The probe was electrically isolated from the probe holder so that contact with the model, for non-spinning runs, could be determined with an ohmmeter. The probe drive mechanism moved the probe perpendicular to the model centerline. In addition, the probe drive mechanism could be positioned circumferentially about the model. Figure 2 shows the model, probe, and probe drive unit installed in the tunnel. Figure 3 is a shadowgraph showing the flow over the model and probe for 4.2 degrees angle of attack.

The boundary layer survey procedure was to bring the impact probe from outside the boundary layer down toward the model and touching it for the no-spin case. Immediately following a no-spin run, the model was brought up to the 333 rps (20,000 rpm) spin rate and the probe was brought down through the boundary layer to within approximately 0.1 mm from the surface. Data were obtained at 3.33, 4.44, and 5.56 calibers (body diameters) from the nose and at angles of attack from 0 to 6.3 degrees. Data were acquired circumferentially in 30 degree increments and also at 10 degrees on each side of the leeward ray (ϕ = 180 degrees). At most positions, surveys were made at both 0 and 333 rps: the spin rate of 333 rps corresponds to a dimensionless spin rate (pd/V) of 0.19 at Mach 3.0. Tunnel conditions for the tests were: Mach 3.0; a supply temperature of 310 K; a supply pressure of 298 kPa. These conditions provided a Reynolds number of 7.3×10^6 based on model length. Local Mach numbers within the boundary layer were determined from the

5. *L. D. Kayser and W. B. Sturek, "Experimental Measurements in the Turbulent Boundary Layer of a Yawed, Spinning Ogive-Cylinder Body of Revolution at Mach 3.0. Part II. Data Tabulation," to be published as a BRL Memorandum Report.*

Rayleigh pitot formula assuming a constant static pressure across the boundary layer. The data in this report were reduced using the experimental values of wall static pressure obtained by Reklis[6]. Figure 4 is a comparison of experimental surface pressures and theoretical surface pressures computed with the inviscid program discussed in the introduction. The model surface temperature was assumed to be equal to the adiabatic wall temperature for turbulent flow and the recovery factor was taken as the cube root of the Prandtl number. The temperature distribution in the boundary layer was found by assuming the Crocco linear total temperature-velocity relationship:

$$\frac{T_t - T_w}{T_o - T_w} = \frac{u}{u_e} .$$

With temperature, pressure, and Mach number known, local values for density and velocity have been computed and tabulated. The integral parameters--displacement thickness, momentum thickness, and velocity thickness--have been computed by integrating the profile data.

The probe axis was aligned longitudinally with the model axis. Some uncertainty is inherent in the profile data due to the probe not being aligned with the local flow direction within the boundary layer. The uncertainty due to cross flow would be of the order of angle of attack at the outer edge of the boundary layer when probing the sides of the model (ϕ = 90 and 270 degrees). The uncertainty due to the effects of spin on the crossflow velocity are expected to be small because the large velocity gradients in a turbulent boundary layer would confine the greatest effect of flow angularity to a very small region near the surface which cannot be probed accurately using a total head probe.

Wall shear stress was obtained for the non-spinning model using the Preston tube technique. The Preston tube is a circular total head probe which is brought down to the model surface and is designed in size to lie within the logarithmic portion of the law-of-the-wall velocity profile. The wall shear stresses are then computed from the Preston tube measurements, the Preston tube size, and model surface pressures using the correlation relations found in reference 7. The free stream Mach number of 3.0 was used in reducing the Preston tube data rather than the local Mach number at the survey station.

6. *R. P. Reklis and W. B. Sturek, "Measurements of Wall Static Pressure on Slender Bodies of Revolution at Angle of Attack," to be published as a BRL Memorandum Report.*

7. *P. Bradshaw and K. Unsworth, "A Note on Preston Tube Calibrations in Compressible Flow," IC Aero Report 73-07, September 1973, Imperial College of Science and Technology, London, Great Britain.*

Data Accuracy -- The pressure transducers are linear to within ± 0.25% of full scale value. The data acquisition system measurement accuracy is approximately 0.1% of full scale. Full scale is rarely achieved on the transducer or the system measurement range; therefore, the accuracy of measured pressures is estimated to be ± 1.0%. Contributing errors in determining the probe height relative to the model surface are as follows: (1) accuracy of probe height calibration; (2) measurement error; and (3) error in determining exactly when the probe contacted the model. The overall accuracy of the probe height value (y-coordinate) is estimated to be within ± 0.1 mm. Values of skin friction obtained by the Preston tube technique are estimated to be accurate to within ± 15%.

III. DISCUSSION OF RESULTS

A summary of test conditions for the SOC boundary layer survey data is given in Table I. A complete set of boundary layer profile data and Preston tube skin friction data are presented in Part II (reference 5) of this report.

To help clarify the data, the orientation of the probe with respect to the model must be known. The circumferential, or azimuthal, position on the model of $\phi = 0$ degrees is defined as the most windward ray on the model when the model is at some angle of attack. Looking upstream at the model base, with the model at positive angle of attack, $\phi = 0$ is on the bottom (6 o'clock); $\phi = 90$ degrees is to the left (9 o'clock); $\phi = 180$ degrees is on the top (12 o'clock); and $\phi = 270$ degrees is to the right (3 o'clock). A clockwise spin is positive; therefore, a positive spin gives a surface velocity in the same direction as cross flow on the left side of the model. On the right side, cross flow and model surface velocities are in the opposite direction. The model coordinate system is shown in Figure 5 with the arrows indicating positive directions.

Figure 6 is a comparison of theoretical and experimental velocity profiles at zero spin and 4.2 degrees angle of attack. This figure illustrates the thickening of the boundary layer when moving from the windward side, $\phi = 0$, to the leeward side, $\phi = 180$. On the leeward side, the theoretical velocities are greater than experimental values near the model surface and the theoretical velocities are smaller than experimental values near the edge of the boundary layer. On the windward side, though not very noticeable, the situation is reversed. The differences in profile shape will give compensating effects when computing integral parameters. Figure 7 is a comparison of theoretical and experimental velocity profiles for the spinning model case. The differences between theory and experiment are virtually the same as for the no-spin case of Figure 6. The effect of spin on experimental velocity profiles is shown in Figure 8 where profiles on the left side of the model are compared with those on the right side. On the wind-

ward side of the model (ϕ = 0 to 90 and 360 to 270), there is almost no measurable effect of spin. However, on the leeward side at ϕ = 120 vs 240 and ϕ = 150 vs 210, the profile shapes differ substantially. The effect of cross flow in opposition (ϕ = 180 to 360) to surface model rotation (e.g. ϕ = 210) is to decrease the fullness of the profile which, of course, will result in a larger displacement thickness. It is also of interest to note that the primary effect of spin is to change the profile shape rather than to change the total thickness.

Values for the longitudinal component of displacement thickness are compared in Figure 9. The agreement between theory and experiment is generally good; however, it is seen at the forward station, ϕ = 0, (Z/D = 3.33) that theoretical thicknesses are slightly greater than experiment and at the aft station theoretical thicknesses are slightly smaller than experiment. This situation indicates that the boundary layer actually grows at a faster rate than predicted by theory; however, this is not particularly surprising since the turbulence model did not provide for any adjustment as a function of pressure gradient. The effect of spin on displacement thickness δ^*_x can be seen in Figure 10 where the increment of δ^*_x due to spin is plotted on an expanded scale for α = 4.2 degrees. The effect on displacement thickness is seen to be significant only in the vicinity of the leeward side (ϕ = 180 degrees). The agreement between theory and experiment is encouraging evidence that the numerical technique accurately models the effect of surface spin.

Measured values for skin friction coefficient obtained using the Preston tube technique are compared to theory in Figure 11. The skin friction coefficient is referenced to free-stream static properties upstream of the model rather than the more conventional approach of using local properties at the edge of the boundary layer. The agreement indicated is within ± 10%. This is considered quite good since the Preston tube is expected to yield an accuracy of ± 10% for two dimensional flat plate boundary layer flow. The use of the Preston tube to obtain measurements in a three dimensional boundary layer flow using two dimensional calibration data must be regarded as speculative and mainly of qualitative interest.

Experimental displacement thickness data at 6.34 degrees angle of attack are shown in Figure 12. The significant difference from the 4.2-degree case is the dip, or decrease, in δ^*_x near the leeward ray (ϕ = 180 degrees). The thicker boundary layers (δ^*_x) on either side of the leeward ray are believed to be caused by the existence of longitudinal separation type vortices which are beginning to develop. Such vortices could create local areas of favorable and adverse pressure gradients that would cause the complexity illustrated in Figure 12. This phenomenon is evidence that conventional boundary layer theory will not be adequate at the higher angles of attack.

IV. CONCLUDING REMARKS

The primary contribution of the experiment described in this report is the unique set of data which can be used to evaluate theoretical computational procedures for three-dimensional turbulent boundary layer development. Analysis of these data and comparisons to theory support the following statements which summarize the primary findings of this report.

(1) The boundary layer data show the effect of spin to be confined primarily to the leeward side of the model.

(2) The excellent agreement between theory and experiment for $\Delta\delta^*_x$ is encouraging evidence that the boundary layer theory accurately models the effects of surface spin.

(3) The circumferential and longitudinal growth of the boundary layer show reasonably good agreement between theory and experiment. However, there is disagreement in the longitudinal growth rate of the boundary layer between theory and experiment.

(4) There is a consistent tendency for the theory to predict a velocity profile that is more full than experiment near the wall and less full than experiment near the edge of the boundary layer.

(5) If the dip in the curve of Figure 12 is an indication of longitudinal development of vortices, significant flow components in the y-direction would exist. Conventional boundary layer equations would not be expected to be valid beyond approximately 5-degrees angle of attack since the equations do not include y-momentum.

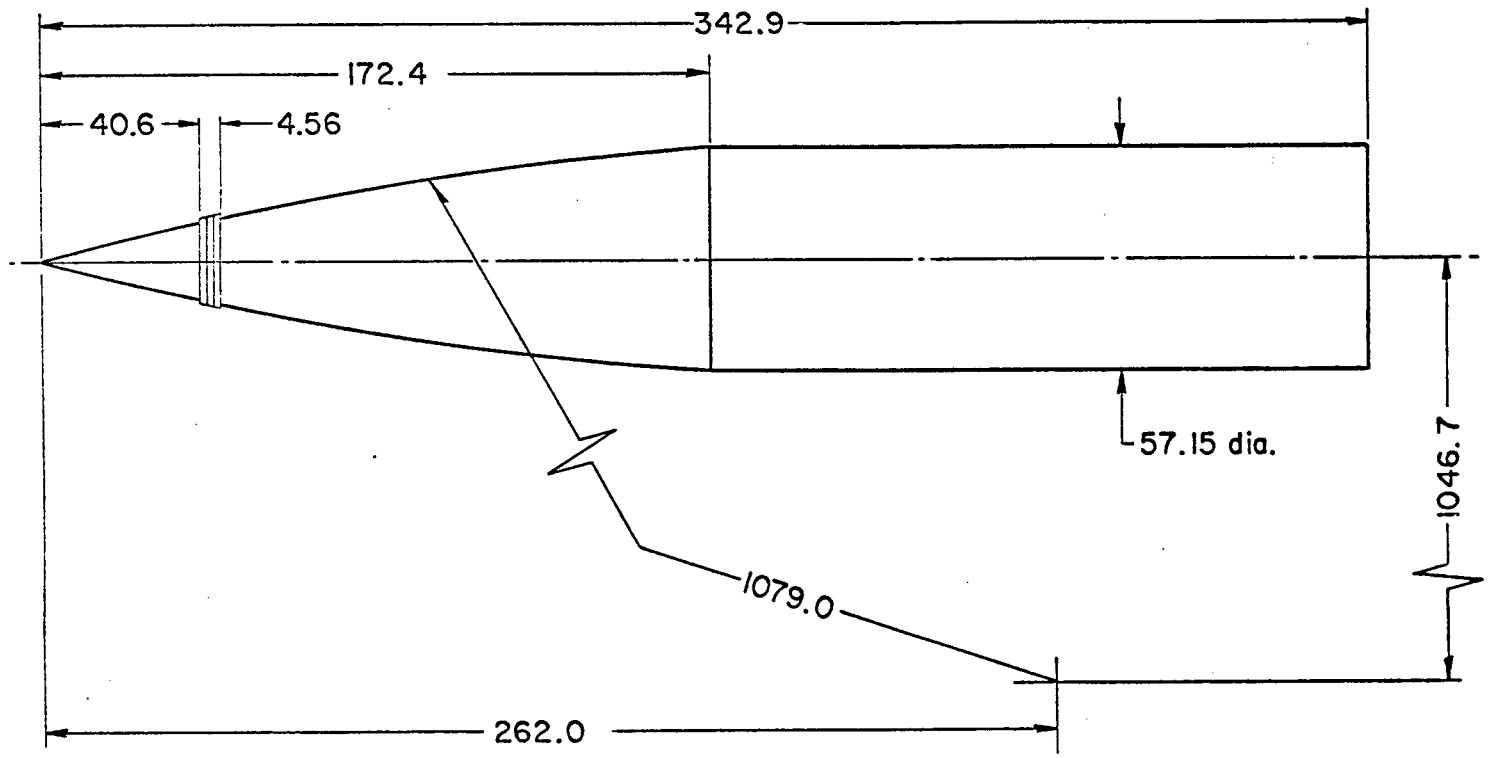

ALL DIMENSIONS IN MILLIMETRES

Figure 1. Model Geometry

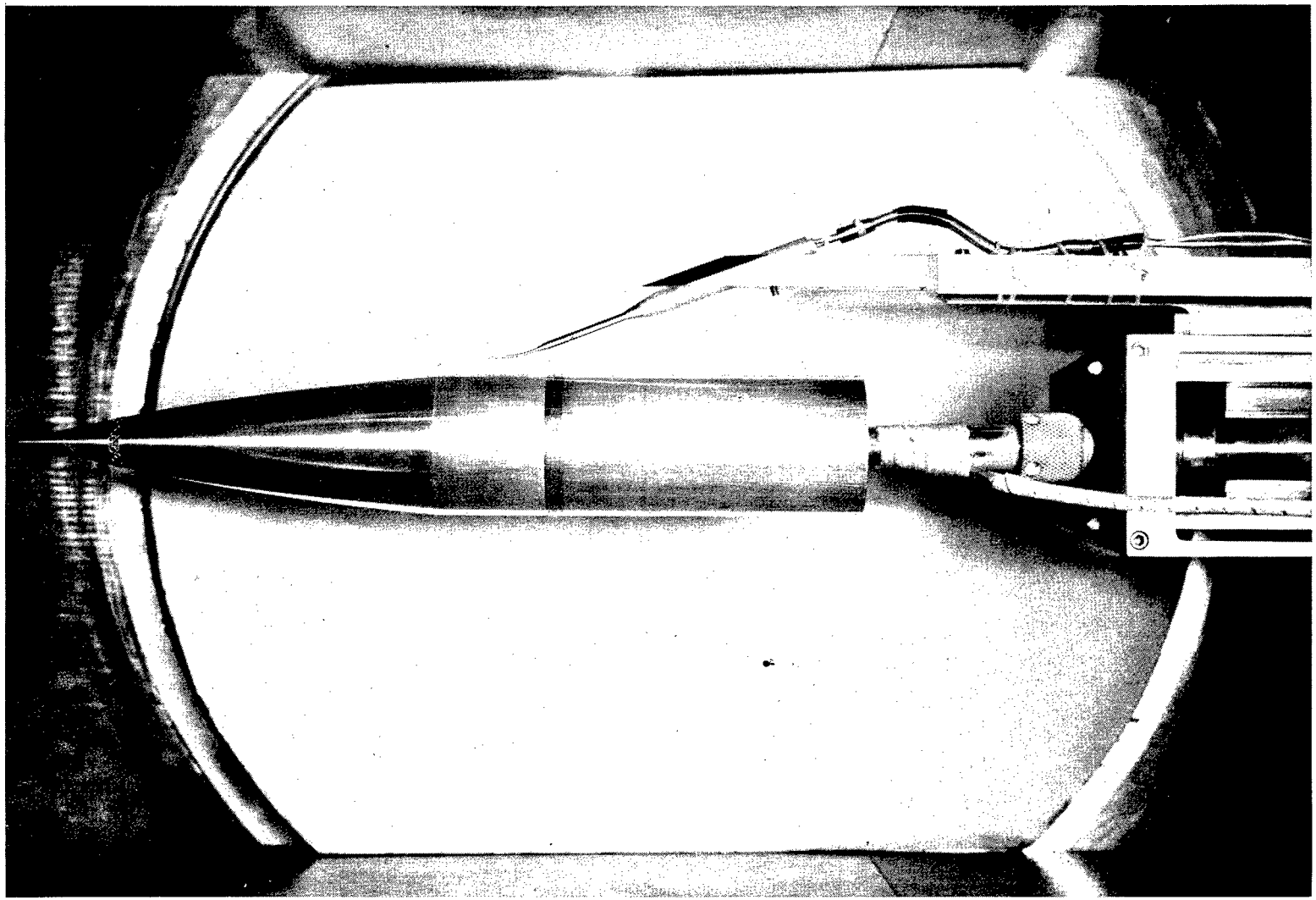

Figure 2. Model Installation Photograph

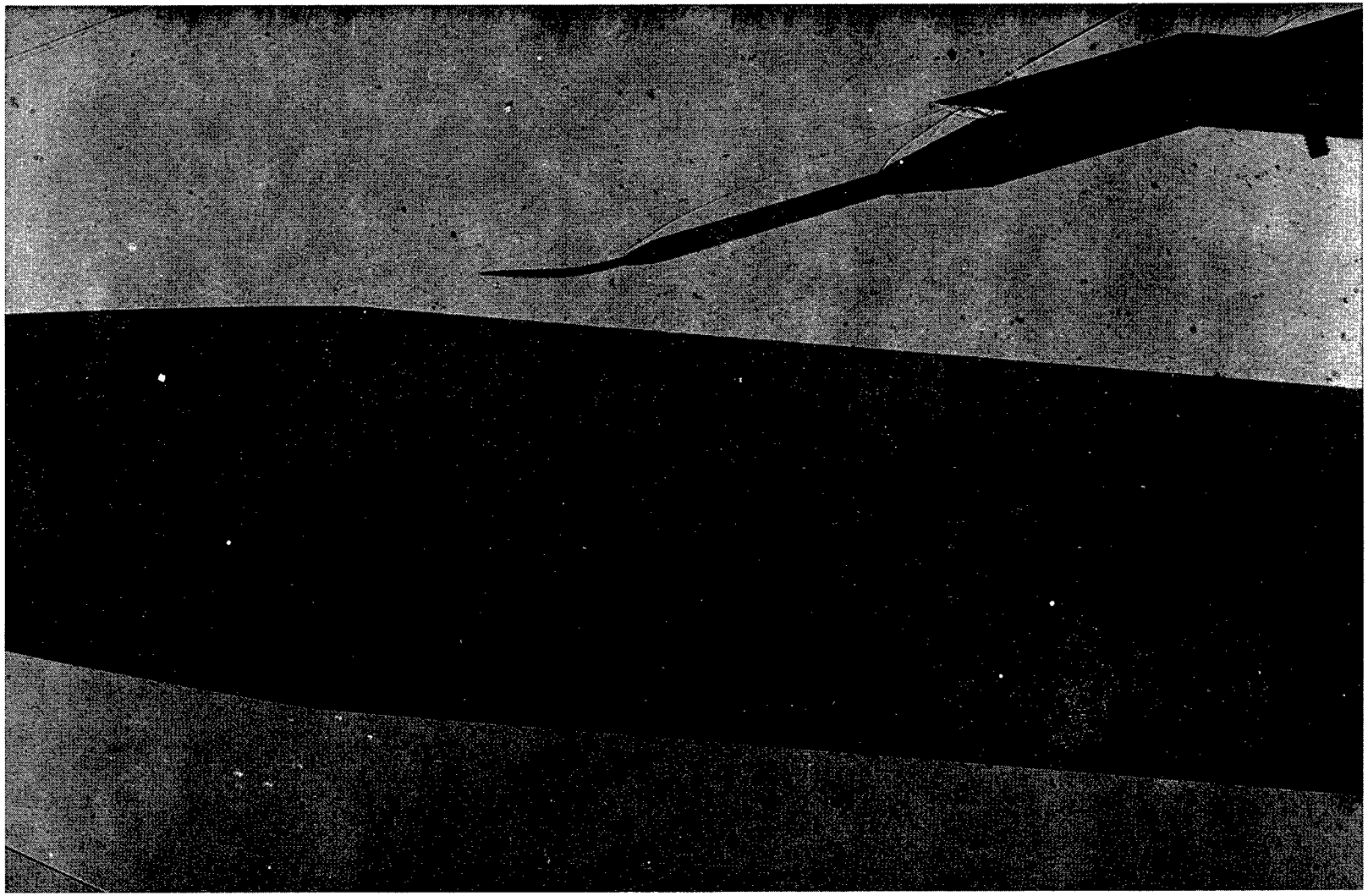

Figure 3. Shadowgraph, α = 4.2 degrees, Z/D = 3.33

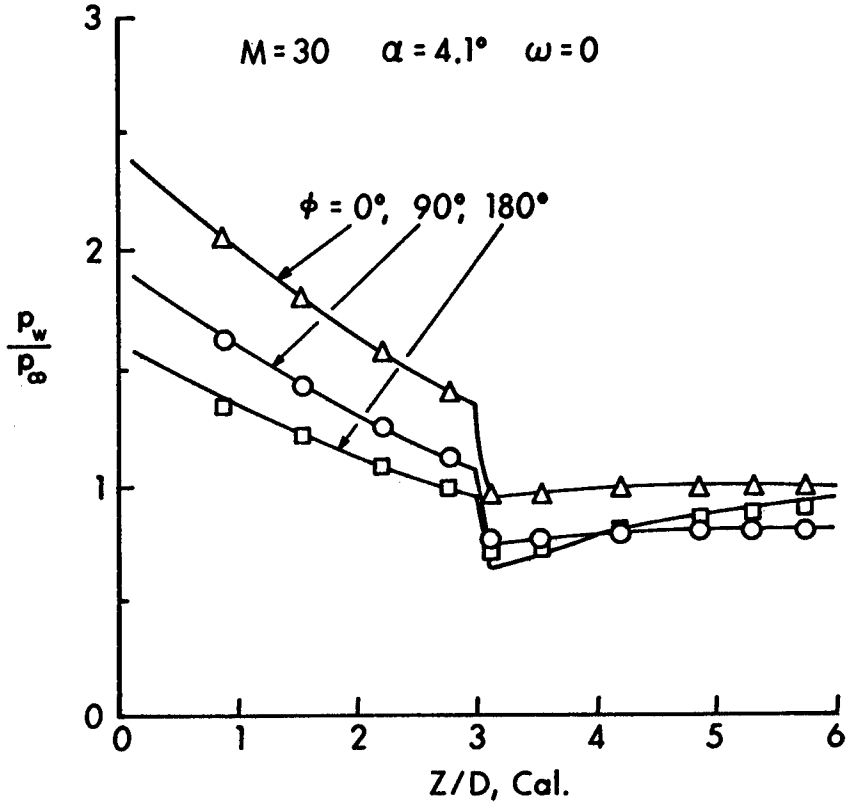

Figure 4. Surface Pressure Distribution on the SOC Model

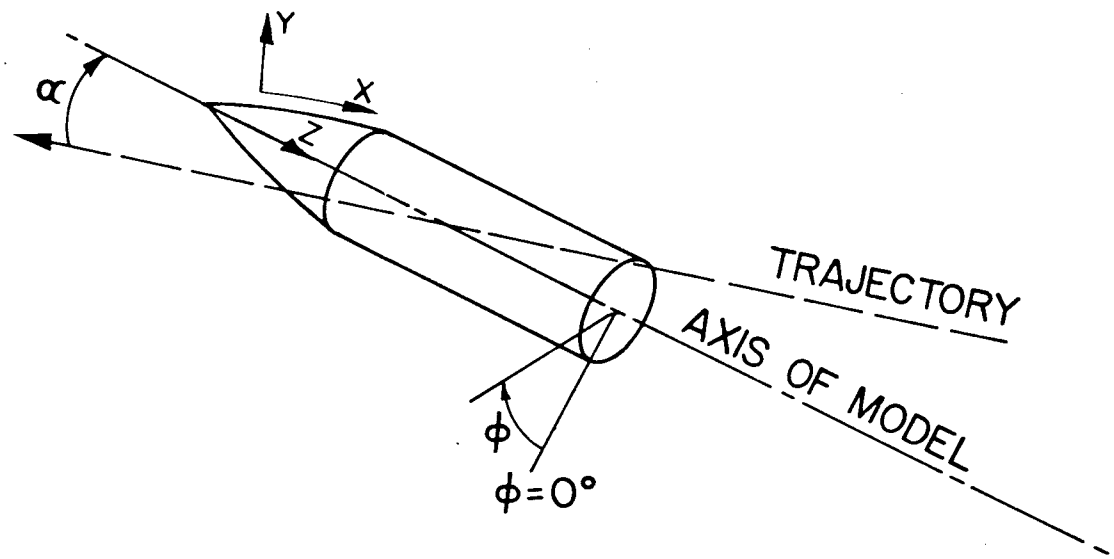

Figure 5. Model Coordinate System

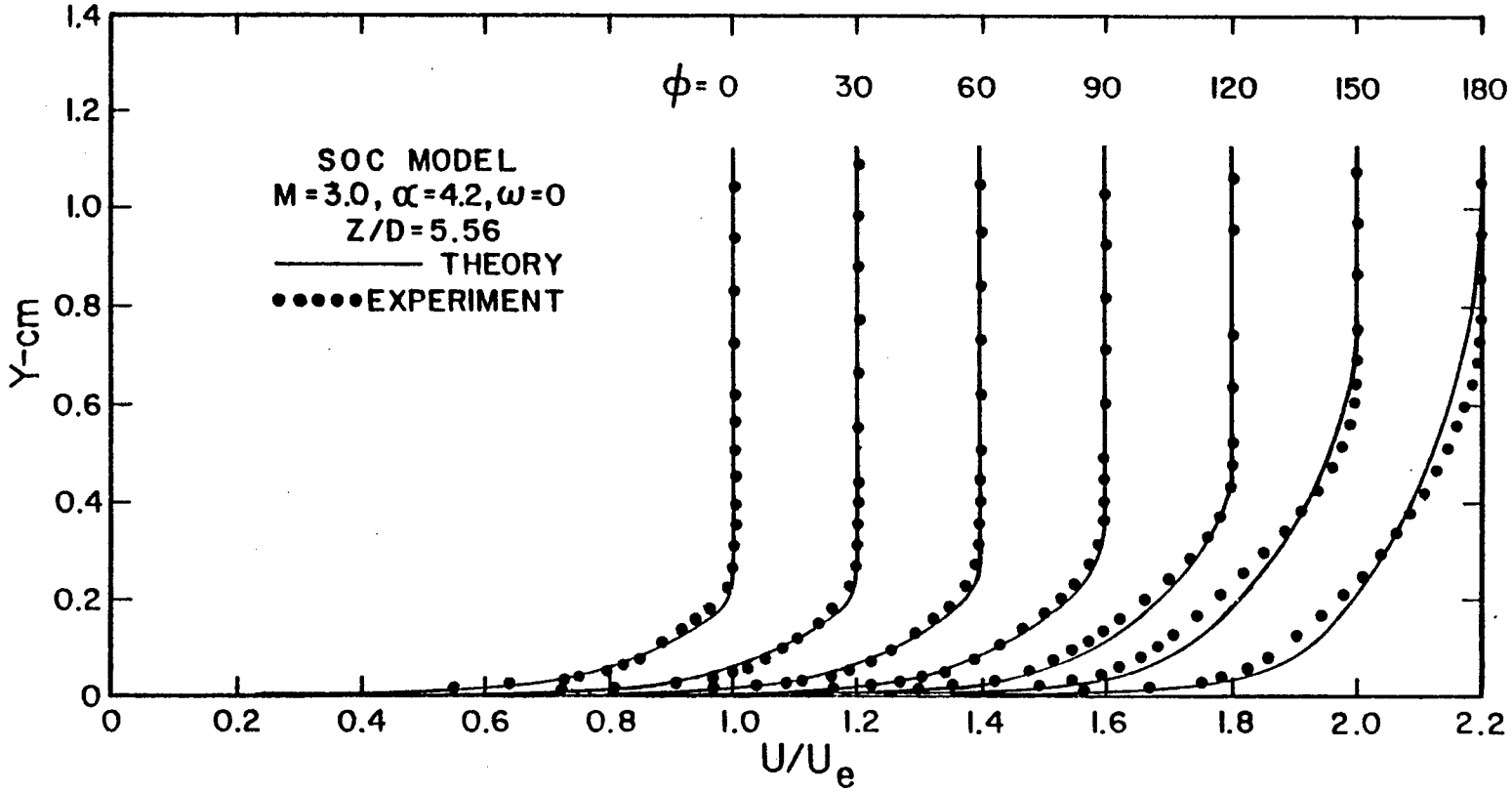

Figure 6. Velocity Profiles, Theory Compared With Experiment

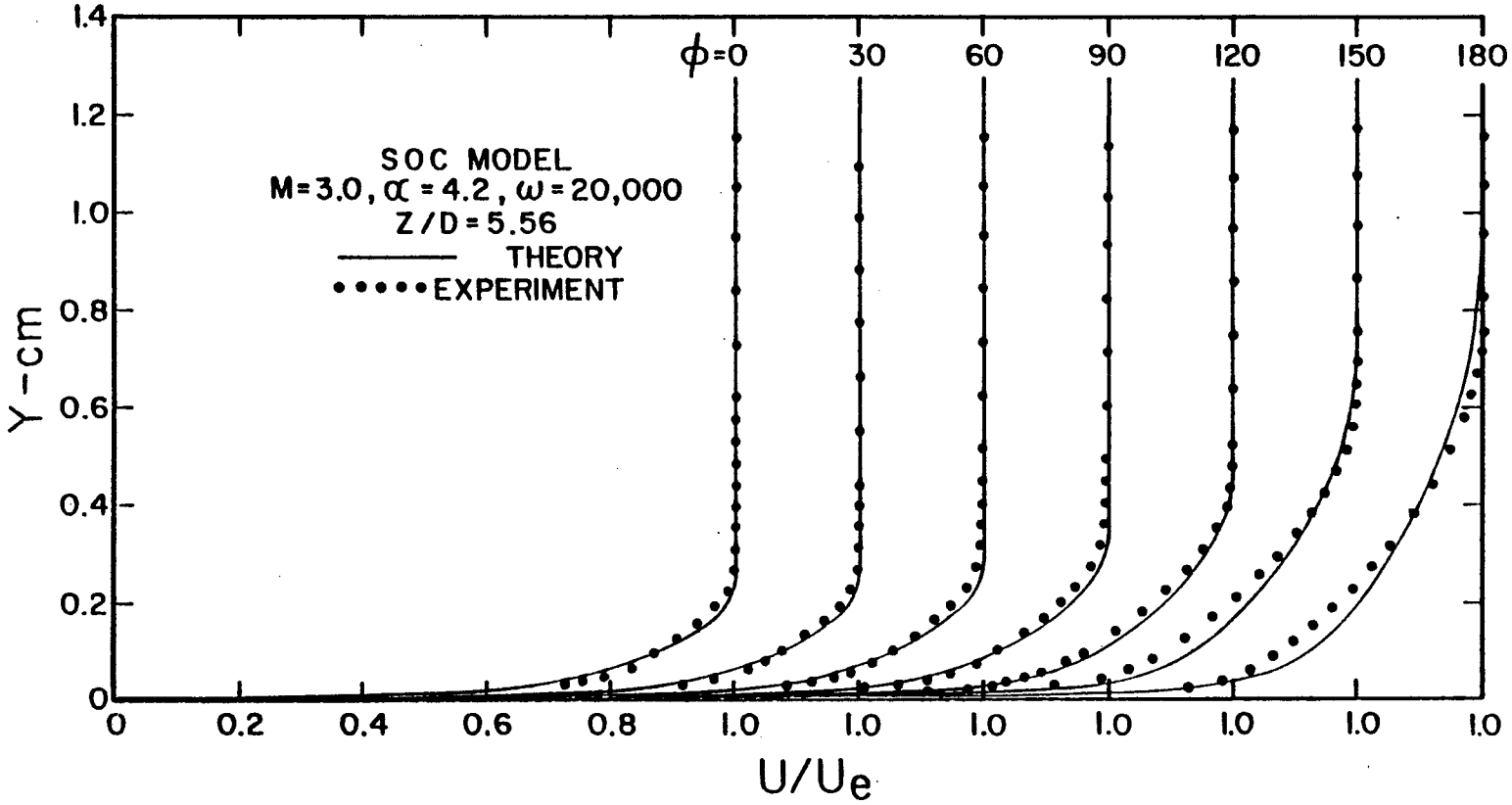

Figure 7. Velocity Profiles, Theory Compared With Experiment

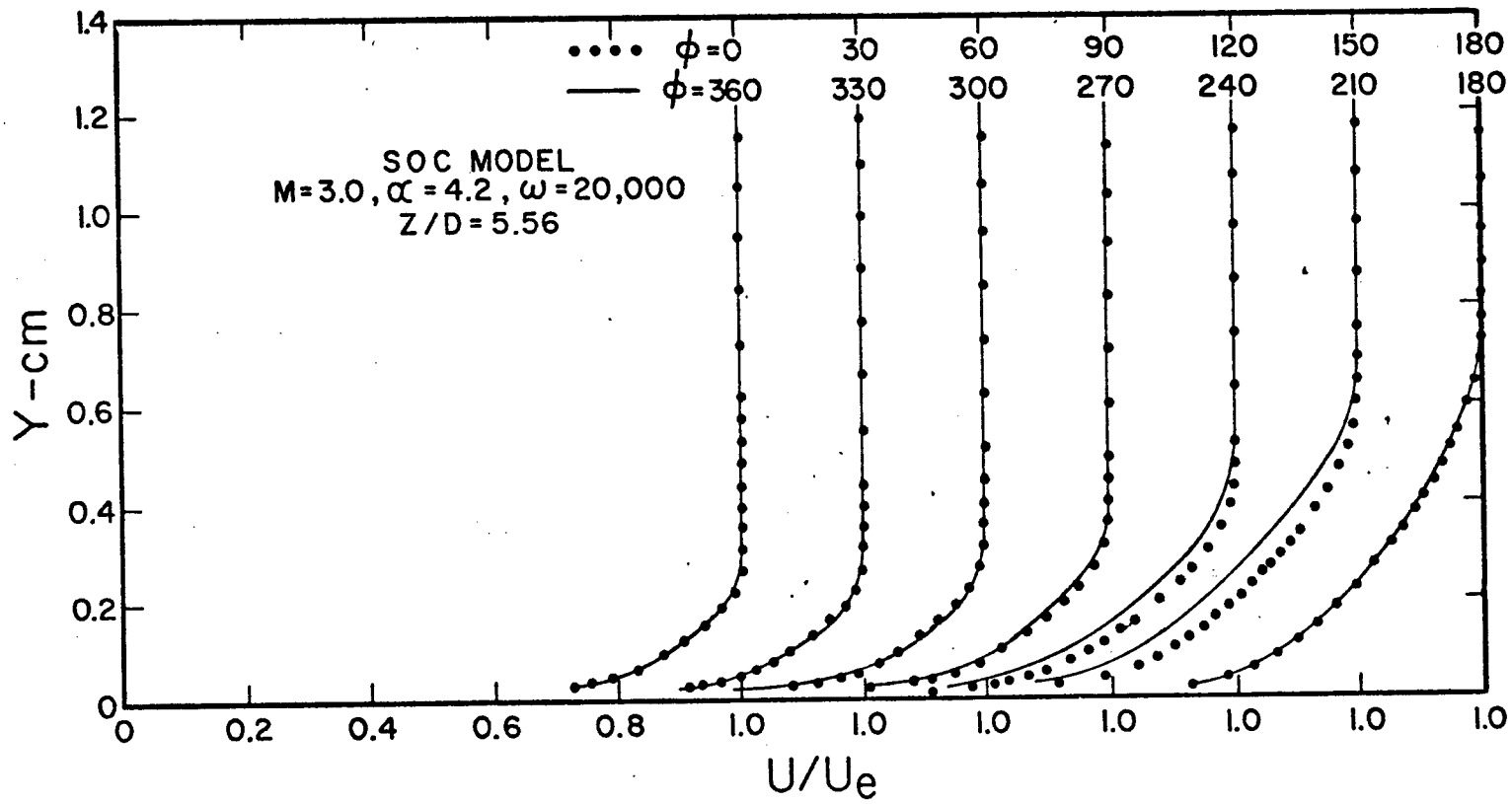

Figure 8. Experimental Velocity Profiles, Effects of Spin

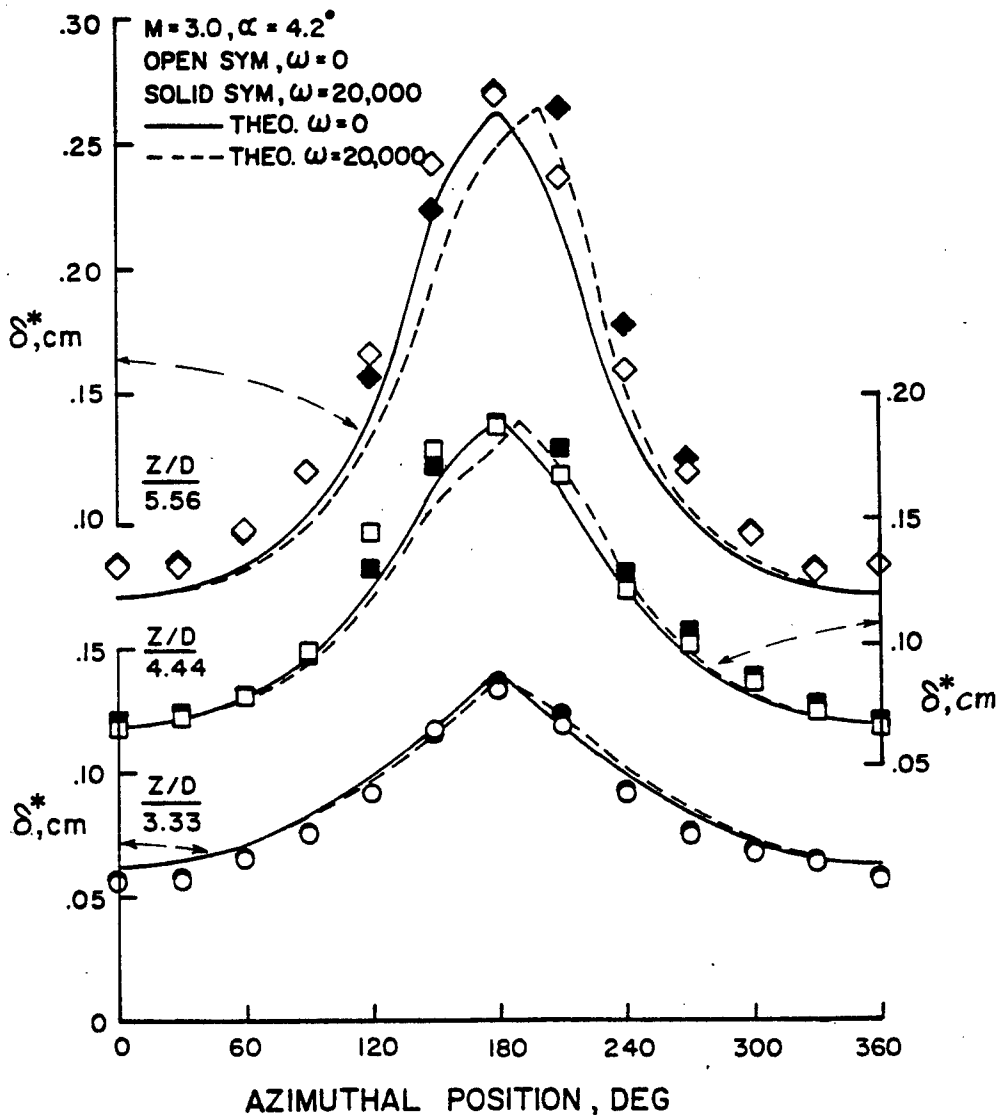

Figure 9. Boundary Layer Displacement Thickness, δ_x^*, Theory and Experiment

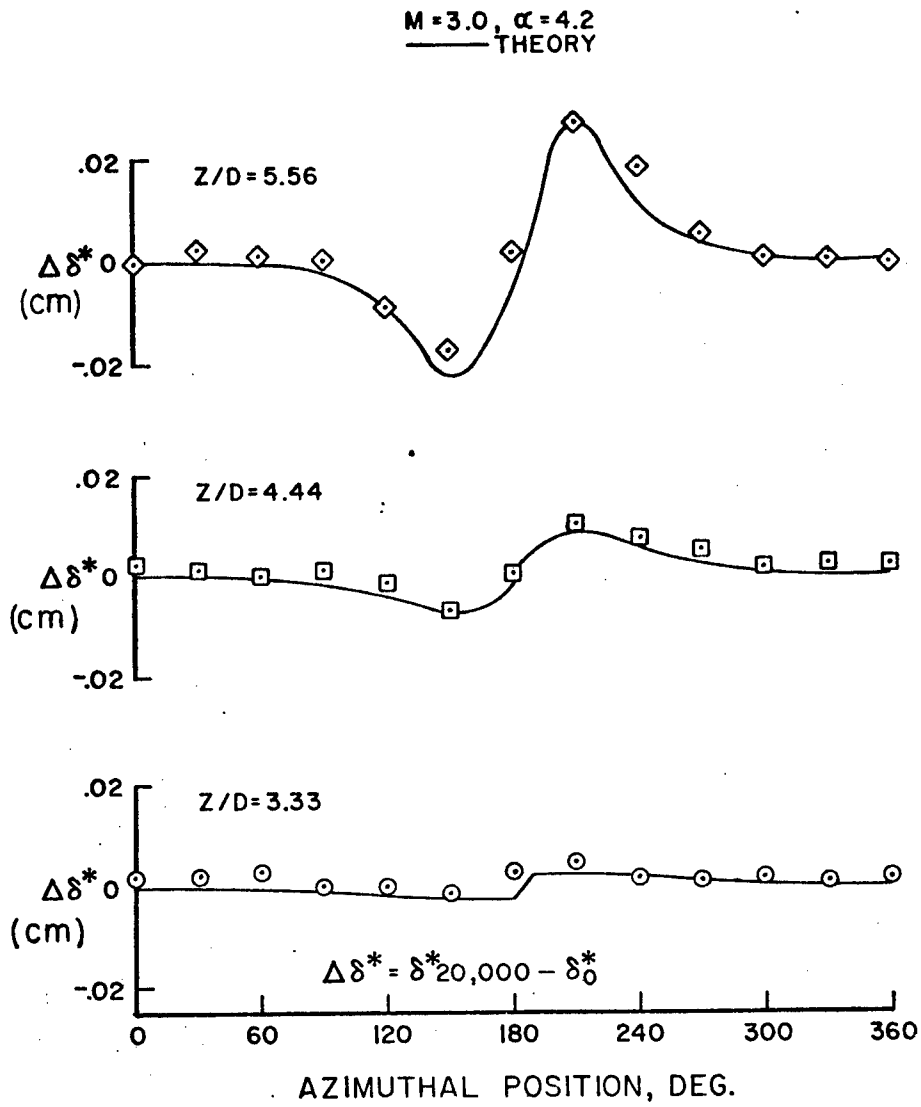

Figure 10. Increment of Displacement Thickness, $\Delta\delta^*_x$, Due to Spin

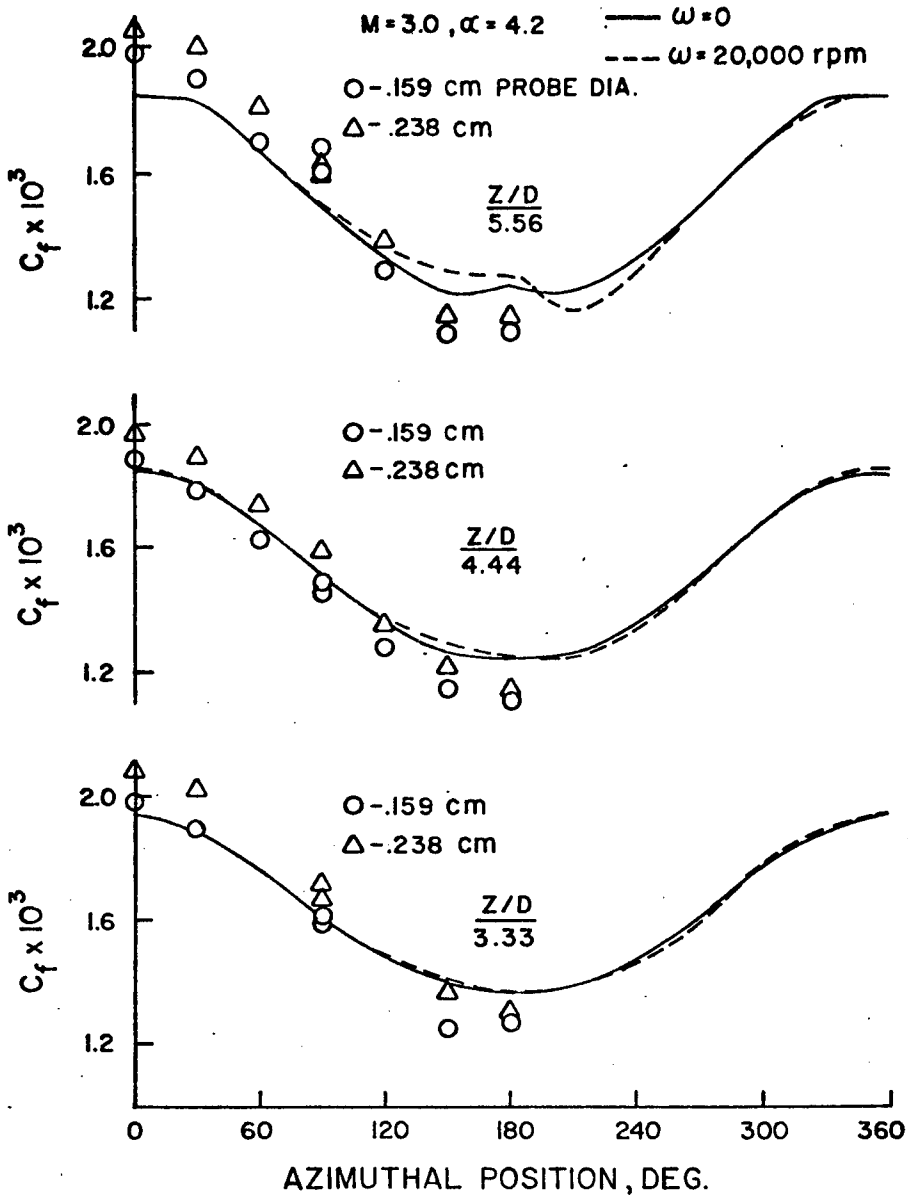

Figure 11. Preston Tube Skin Friction Results

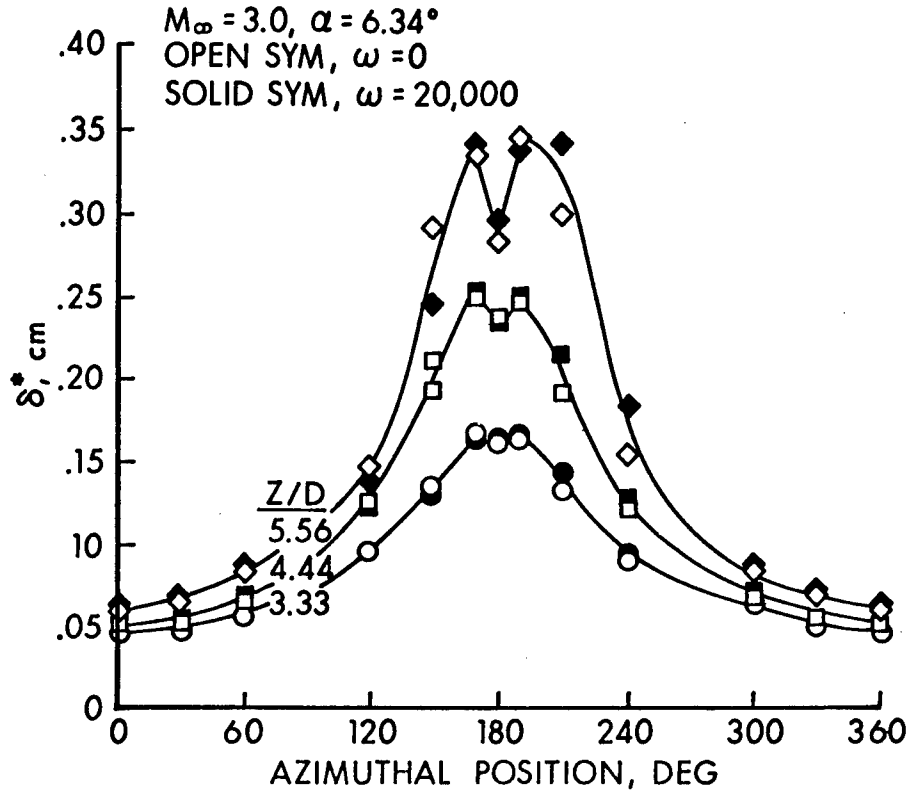

Figure 12. Experimental Displacement Thicknesses, α = 6.3 Degrees

Table 1. Test Run Summary

Z/D = 3.33

ϕ	$\alpha = 0$	$\alpha = 2.1$	$\alpha = 4.2$	$\alpha = 5.3$	$\alpha = 6.3$
0	0	0,333*	0,333		0,333
30	0	0,333	0,333		333
60	0	0,333	0,333		0,333
90	0	0,333	0,333		
120		0,333	0,333	0,333	0,333
150		0,333	0,333	0,333	0,333
170		0,333	0,333	0,333	0,333
180		0,333	0,333	0,333	0,333
190		0,333	0,333	0,333	0,333
210		0,333	0,333	0,333	0,333
240		0,333	0,333	0,333	0,333
270		0,333	0,333		
300		0,333	0,333		0,333
330		0,333	0,333		0,333

Z/D = 4.44

0	0	0,333	0,333		0,333
30	0	0,333	0,333		0,333
60	0	0,333	0,333		0,333
90	0	0,333	0,333		
120		0,333	0,333	0,333	0,333
150		0,333	0,333	0,333	0,333
170		0,333	0,333	0,333	0,333
180		0,333	0,333	0,333	0,333
190		0,333	0,333	0,333	0,333
210		0	0,333	0,333	0,333
240		0,333	0,333	0,333	0,333
270		0,333	0,333		
300		0,333	0,333		0,333
330		0,333	0,333		0

Table 1. Test Run Summary (Continued)

ϕ	$\alpha = 0$	$\alpha = 2.1$	$\alpha = 4.2$	$\alpha = 5.3$	$\alpha = 6.3$
			Z/D = 5.56		
0	0	0,333*	0,333		0,333
30	0	0,333	0,333		0,333
60	0	0,333	0,333		0,333
90	0	0,333	0,333		
120		0,333	0,333		0,333
150		0,333	0,333	0,333	0,333
170		0,333	0,333	0,333	0,333
180		0,333	0,333		0,333
190		0,333	0,333	0,333	0,333
210		0,333	0,333	0,333	0,333
240		0,333	0,333	0,333	0,333
270		0	0,333		
300		0,333	0,333		0,333
330		0,333	0,333		0,333

* Model Spin Rate, 0 and 333 rps, 333 rps = 20,000 rpm

REFERENCES

1. H. A. Dwyer, "Three Dimensional Flow Studies Over a Spinning Cone at Angle of Attack," BRL Contract Report No. 137, February 1974, U.S. Army Ballistic Research Laboratory, Aberdeen Proving Ground, Maryland. AD 774795.

2. H. A. Dwyer and B. R. Sanders, "Magnus Forces on Spinning Supersonic Cones. Part I: The Boundary Layer," BRL Contract Report No. 248, July 1975, U.S. Army Ballistic Research Laboratory, Aberdeen Proving Ground, Maryland. AD A013518. Also, *AIAA Journal*, Vol. 14, No. 4, April 1976, p. 498.

3. B. R. Sanders, "Three-Dimensional, Steady, Inviscid Flow Field Calculations With Application to the Magnus Problem," PhD Dissertation, University of California, Davis, California, May 1974.

4. W. B. Sturek (et al), "Computations of Turbulent Boundary Layer Development Over a Yawed, Spinning Body of Revolution With Application to Magnus Effect," BRL Report No. 1985, May 1977, U.S. Army Ballistic Research Laboratory, Aberdeen Proving Ground, Maryland. AD A041338.

5. L. D. Kayser and W. B. Sturek, "Experimental Measurements in the Turbulent Boundary Layer of a Yawed, Spinning Ogive-Cylinder Body of Revolution at Mach 3.0. Part II. Data Tabulation," to be published as a BRL Memorandum Report.

6. R. P. Reklis and W. B. Sturek, "Measurements of Wall Static Pressure on Slender Bodies of Revolution at Angle of Attack," to be published as a BRL Memorandum Report.

7. P. Bradshaw and K. Unsworth, "A Note on Preston Tube Calibrations in Compressible Flow," IC Aero Report 73-07, September 1973, Imperial College of Science and Technology, London, Great Britain.

LIST OF SYMBOLS

c_f	skin friction coefficient, τ_w/q_∞
d,D	diameter of model base, mm
p	model spin rate, radians/second
p_{t_2}	impact probe pressure, kPa
p_w	model wall static pressure, kPa
p_∞	free-stream static pressure, kPa
q_∞	free-stream dynamic pressure, kPa
SOC	secant-ogive-cylinder
T_o	tunnel total temperature, K
T_t	local total temperature, K
T_w	model wall temperature, K
u,w,v	velocities in boundary layer coordinates, m/s
u_e	velocity at edge of boundary layer, m/s
V	velocity along model trajectory, m/s
x,ϕ,y	boundary layer coordinates, Figure 5
z,Z	longitudinal model axis coordinate, mm
α	angle of attack, degrees
δ_x^*	longitudinal component of displacement thickness, cm
$\Delta\delta_x^*$	increment of displacement thickness due to spin, cm
τ_w	model wall shear stress, N/m^2
ϕ	circumferential boundary layer coordinate, degrees

DISTRIBUTION LIST

No. of Copies	Organization
12	Commander Defense Documentation Center ATTN: DDC-TCA Cameron Station Alexandria, Virginia 22314
1	Commander US Army Materiel Development and Readiness Command ATTN: DRCDMA-ST 5001 Eisenhower Avenue Alexandria, Virginia 22333
1	Commander US Army Aviation Research and Development Command ATTN: DRSAV-E 12th and Spruce Streets St. Louis, Missouri 63166
1	Director US Army Air Mobility Research and Development Laboratory Ames Research Center Moffett Field, CA 94035
1	Commander US Army Electronics Command ATTN: DRSEL-RD Fort Monmouth, NJ 07703
1	Commander US Army Jefferson Proving Ground ATTN: STEJP-TD-D Madison, Indiana 47250
5	Commander US Army Missile Research and Development Command ATTN: DRDMI-R DRDMI-T DRDMI-TD Mr. R. Becht Mr. R. Deep Dr. D. Spring Redstone Arsenal, AL 35809
1	Commander US Army Tank Automotive Research and Development Command ATTN: DRDTA-RWL Warren, Michigan 48090
2	Commander US Army Mobility Equipment Research and Development Command ATTN: Tech Docu Cen, Bldg. 315 DRSME-RZT Fort Belvoir, Virginia 22060
1	Commander US Army Armament Materiel Readiness Command ATTN: DRSAR-LEP-L, Tech Lib Rock Island, Illinois 61202
3	Commander US Army Armament Research and Development Command ATTN: DRDAR-LCA-F Mr. D. Mertz Mr. E. Falkowski Mr. A. Loeb Dover, New Jersey 07801
1	Commander US Army Harry Diamond Labs. ATTN: DRXDO-TI 2800 Powder Mill Road Adelphi, Maryland 20783

DISTRIBUTION LIST

No. of Copies	Organization
1	Director US Army TRADOC Systems Analysis Activity ATTN: ATAA-SL, Tech Lib White Sands Missile Range NM 88002
1	Commander US Army Research Office P. O. Box 12211 Research Triangle Park NC 27709
2	Commander David W. Taylor Naval Ship Research & Development Ctr ATTN: Dr. S. de los Santos Mr. Stanley Gottlieb Bethesda, MD 20084
1	Commander US Naval Surface Weapons Ctr ATTN: Dr. T. Clare, Code DK20 Dahlgren, VA 22448
4	Commander US Naval Surface Weapons Ctr ATTN: Code 312, Mr.S.Hastings Code 313, Mr. R. Lee Mr. W. Yanta Mr. R. Voisinet Silver Spring, MD 20910
1	AEDC (Mr. J. Whitfield) Arnold AFS, TN 37389
1	New York State Energy Research and Development Authority ATTN: Dr. Irwin E. Vas 230 Park Avenue New York, NY 10017
8	Director NASA Ames Research Center ATTN: MS-202-1, Dr. H. Lomax Dr. R. MacCormack Dr. J. Steger Dr. L. Schiff Dr. C. M. Hung Dr. J. Rakich MS-229-1, Dr. J. Marvin Dr. R. Agarwal Moffett Field, CA 94035
2	Director NASA Langley Research Center ATTN: MS 185, Tech Lib MS 161, Mr. D. Bushnell Langley Station Hampton, VA 23365
1	Arnold Research Organization, Inc. von Karman Gas Dynamics Facility ATTN: Dr. John C. Adams, Jr. Aerodynamics Division Projects Branch Arnold AFS, TN 37389
2	Aeronutronic Division Aeronutronic Ford Corporation ATTN: Dr. A. Demetriades Dr. A. Laderman Ford Road Newport Beach, CA 92663
1	Douglas Aircraft Company McDonnell-Douglas Corporation ATTN: Dr. Tuncer Cebeci 3855 Lakewood Boulevard Long Beach, CA 90801

DISTRIBUTION LIST

No. of Copies	Organization
1	Sandia Laboratories ATTN: Dr. F. G. Blottner P. O. Box 5800 Albuquerque, NM 87115
1	Princeton University James Forrestal Research Ctr Gas Dynamics Laboratory ATTN: Prof. S. Bogdonoff Princeton, NJ 08540
1	University of California Dept of Mechanical Engineering ATTN: Prof. H. A. Dwyer Davis, CA 95616
1	Polytechnic Institute of New York ATTN: Dr. S. G. Rubin Farmingdale, NY 11735
1	University of Delaware Mechanical and Aerospace Engineering Department ATTN: Dr. James E. Danberg Newark, DE 19711
2	University of Virginia Department of Aerospace Engineering and Engineering Physics ATTN: Prof. I. Jacobson Prof. J. B. Morton Charlottesville, VA 22904
	Aberdeen Proving Ground
	Marine Corps Ln Ofc Dir, USAMSAA